A Study of the Electronic and Geometric Structure of Colloidal $Ti^0 \cdot 0.5THF$

R. Franke,† J. Rothe,† J. Pollmann,† J. Hormes,*,† H. Bönnemann,*,‡ W. Brijoux,‡ and Th. Hindenburg‡

Contribution from the Physikalisches Institut, Universität Bonn, Nussallee 12, D-53115 Bonn, Germany, and Max-Planck-Institut für Kohlenforschung, Postfach 101353, D-45466 Mülheim an der Ruhr, Germany

Received October 20, 1995[⊗]

Abstract: The reduction of $TiBr_4 \cdot 2THF$ using $K[BEt_3H]$ yields the hydrogen-free organosol $Ti \cdot 0.5THF$. According to the HRTEM (high-resolution transmission electron microscopy), EDX (energy-dispersive X-ray) fluorescence, XPS (X-ray photoelectron spectroscopy), XANES (X-ray absorption near edge structure), and EXAFS (extended X-ray absorption fine structure) data, this nanoparticulate metal colloid consists of very small Ti particles in the zerovalent state, stabilized by intact THF molecules.

Introduction

Recently we have communicated the existence of an ether-soluble "TiH_2" obtained from the reduction of $TiCl_4$ with the borate $[BEt_3H]^-$, which produces H_2 when dried, to give a zerovalent colloidal Ti containing (besides KCl) various amounts of included residual hydrogen.[1] Here we report on the synthesis and give a detailed physical characterization of a hydrogen-free colloid $[Ti \cdot 0.5THF]_x$ (THF = tetrahydrofuran). The use of $TiBr_4 \cdot THF$ as the starting material for the reduction and subsequent cooling of the reaction mixture to −78 °C allows 99% of the KBr to be removed from the product. In vacuo (10^{-3} mbar) H_2 and BEt_3 may be completely removed together with the solvent:[2]

$$TiBr_4 \cdot 2THF + 4K[BEt_3H] \xrightarrow[\substack{1.\ 2\ h,\ 20\ °C \\ 2.\ 16\ h,\ -78\ °C}]{THF} [Ti \cdot 0.5THF]_x + 4BEt_3 + 4KBr\downarrow + 2H_2\uparrow$$

1

The isolated organosol **1** is extremely oxophilic, very soluble in THF, but insoluble in hydrocarbons. Protonolysis of **1** with 2 N HCl gave 1.5 mol of H_2/mol of Ti, indicating that no residual hydrogen was present. No particles were detectable using HRTEM (high-resolution transmission electron microscopy), indicating a size below 0.8 nm. The IR (infrared) spectroscopy and NMR (nuclear magnetic resonance) spectroscopy data confirm that intact THF is coordinated to the metallic center (see the Results).

To obtain more detailed information about the chemical state and the average coordination number of the metal atoms, about interatomic distances, and about the interaction between the metallic center and the stabilizing THF ligands, these extremely small particles were studied using XPS (X-ray photoelectron spectroscopy) and XAS (X-ray absorption spectroscopy). Both techniques have proven to be powerful tools for the investigation of the electronic and geometric structure of small metallic clusters in the absence of well-defined crystal structure.[3,4]

The spectroscopic features near the absorption edge (XANES = X-ray absorption near edge structure) represent electronic transitions from a core level into unoccupied electronic bands or orbitals. From the presence, the intensity, and the energy position of distinct absorption features information about the chemical state and the geometry of the coordination polyhedron of the absorbing atoms can be derived. Also changes of the electronic band structure of small particles compared with the bulk metal can be studied. The analysis of the oscillatory part of the absorption spectra up to 1000 eV above the edge position, called EXAFS (extended X-ray absorption fine structure), allows the determination of the average coordination number of the atom under consideration and the type and the distances of neighbor atoms.[5]

XPS measurements yield quantitative and qualitative information about the chemical composition of the sample under investigation.[6] Since the mean free path length of the photoelectrons emitted from condensed matter is limited, both types of information are surface sensitive. It is well known that the energy position of a signal measured in XPS is affected by the chemical state of the atom under consideration.[6,7] The magnitude of the resulting chemical shift, $\Delta E(i)$, of electron binding energies (BE) observed from sample to sample or by referring to the corresponding elemental solid characterizes the charge state of the element under consideration.

In this paper we report on the XPS and XAS investigation of **1**. The results obtained from a comparison with the spectra of suitable reference samples such as Ti metal and several crystalline Ti oxides support the presence of very small Ti^0 particles interacting with coating THF molecules.

* To whom correspondence should be addressed.
† Universität Bonn.
‡ Max-Planck-Institut für Kohlenforschung.
⊗ Abstract published in *Advance ACS Abstracts*, November 1, 1996.

(1) (a) Bönnemann, H.; Korall, B. *Angew. Chem.* **1992**, *104*, 1506−1508; *Angew. Chem., Int. Ed. Engl.* **1992**, *31*, 1490−1492. (b) Bönnemann, H.; Brijoux, W.; Brinkmann, R.; Fretzen, R.; Joußen, T.; Köppler, R.; Korall, B.; Neiteler, P.; Richter, J. *J. Mol. Catal.* **1994**, *86*, 129−177. (c) Bönnemann, H.; Brijoux, W. *Mater. Res. Soc. Symp. Proc.* **1994**, *351*, 3−14. (d) Bönnemann, H.; Brijoux, W. *Nanostruct. Mater.* **1995**, *5*, 135−140. (e) Bönnemann, H.; Brijoux, W. In *Studies in Surface Science and Catalysis*; Poncelet, G., Ed.; Elsevier: Amsterdam, 1995; pp 185−195.

(2) Hindenburg, Th. Ph.D. Thesis, RWTH Aachen, 1995.

(3) (a) Apai, G.; Lee, S. T.; Mason, M. G.; Gerenser, L. J.; Gardner, S. A. *J. Am. Chem. Soc.* **1979**, *101*, 6880−6883. (b) Moretti, G.; Porta, P. *Surf. Sci.* **1993**, *287/288*, 1076−1081.

(4) (a) Mansour, A. N.; Cook, J. W., Jr.; Sayers, D. E. *J. Phys. Chem.* **1984**, *88*, 2330−2334. (b) Sinfelt, J. H.; Via, G. H. *Catal. Rev.−Sci. Eng.* **1984**, *26*, 81−140. (c) Montano, P. A., Cao, Y. *J. Phys.: Condens. Matter* **1993**, *5*, A209−A210.

(5) Koningsberger, D. C., Prins, R., Eds.; *X-ray Absorption: Techniques of EXAFS, SEXAFS and XANES*; John Wiley & Sons: New York, 1988.

(6) Briggs, D., Seah, M. P., Eds. *Practical Surface Analysis by Auger and X-ray Photoelectron Spectroscopy*; Wiley: Chicester, 1983.

(7) Egelhoff, W. F., Jr. *Surf. Sci. Rep.* **1987**, *6−8*, 253−415.

S0002-7863(95)03525-6 CCC: $12.00

Experimental Section

A. Preparation of 1 [[Ti·0.5THF]$_x$]. A 70 mL sample of a 1.15 M solution of K[BEt_3H] (80 mmol) in THF was added at room temperature (rt) over 2 h to a stirred suspension of $TiBr_4$·2THF (10.24 g, 20 mmol) in THF. During the reduction approximately 20 mmol of H_2 was released. The reaction mixture was stirred for another 2 h at rt. The precipitated KBr was removed by filtration. BEt_3 and THF were removed from the brown filtrate in vacuo (10^{-3} mbar). The product was dried in vacuo for 16 h. Yield: **1**, 1.61 g (79%); KBr, 9.39 g (99%). Elemental analysis: Ti, 38.9%; K, 5.5%; Br, 0.7%. EDX (energy-dispersive X-ray) fluorescence area analysis confirmed the Ti: halide ratio found by elemental analysis.

All manipulations were carried out in an Ar atmosphere using Schlenck techniques. The solvents were dried and distilled under Ar. The transfer of the samples into special holders for XPS and XAS was carried out in a glovebox (O_2, H_2O, <1 ppm).

B. IR/NMR/TEM. IR spectra were obtained using KBr pellets in a Nicolet FT-IR 7199 spectrometer. NMR spectra were recorded on a Bruker MC200 (200.1 MHz for ^1H) spectrometer. TEM images were taken with a Hitachi HF2000 high-resolution TEM at an acceleration voltage of 200 keV.

C. X-ray Photoelectron Spectroscopy. The XPS measurements were performed using a concentric hemispherical electron-energy analyzer (CLAM 2, FISONS Instruments) working in the constant pass-energy mode (50 eV). The spectra were excited with an X-ray tube (XR2, FISONS Instruments) equipped with an Al/Mg twin anode working at 12 kV and 300 W. The energy scale of the spectrometer was calibrated by recording the Cu $2p_{3/2}$ (932.65 eV) and the Au $4f_{7/2}$ (84.0 eV) lines[8] originating from a standard sample. In this paper we report on XPS data from a cleaned Ti metal sample to compare the colloid results with those from bulk metal. The cleaning of the Ti metal surface was performed by means of Ar sputtering at 3 keV and about 20 μA (Microetch, Oxford Applied Research) for 2 and 4 h, respectively.

All electron binding energies presented here are referenced to the Au $4f_{7/2}$ energy (84.0 eV[8]) obtained from an admixture of gold powder to the samples. The detail spectra (Ti 2p; O 1s) were analyzed by means of a least-squares fitting routine using Voigt profiles.[9]

D. X-ray Absorption Spectroscopy. The XAS measurements at the Ti K-edge (~4966 eV) were performed in the beamline BN3 at the Synchrotron Radiation Laboratory of the electron stretcher and accelerator (ELSA), Institute of Physics, Bonn University.[10] The ELSA was operated in storage-ring mode at an energy of 2.3 GeV and an average current of 40 mA. Synchrotron radiation was monochromatized by means of a double-crystal monochromator (Lemonnier type[11]) equipped with two plane Ge(220) crystals. By fitting a Voigt profile to the pre-edge resonance at about 4966 eV in the Ti K-XANES spectrum of $TiCl_4$, a monochromator resolution of about 0.9 eV was determined.

The reported spectra were recorded using the transmission technique with ionization chambers for detecting both the primary and the transmitted beam intensities. The energy scale of the monochromator was calibrated after each measurement of a Ti compound by aligning the first inflection point in the absorption spectrum of a 7.5 μm thick Ti reference foil (Ti K-edge) to 4966 eV.[12] All the reported XANES spectra are referenced to this assignment.

Three different step widths were chosen: 1.1 eV/step from 4900 to 4950 eV (pre-edge region), 0.11 eV/step from 4950 to 5000 eV (near-edge), and 0.8 eV/step from 5000 to 5600 eV (EXAFS). To compare the XANES spectra of the Ti colloid and the reference samples quantitatively, a linear background was fitted to the pre-edge region (4900−4950 eV) and subtracted before the normalization of the spectra with respect to the absorption jump. Due to the oxophilic character of the Ti colloid the XPS and XAS investigations required a sample-preparation technique under perfect inert-gas conditions. The details of the sample preparation are described in ref 13. Note that the Ti colloid was studied as synthesized (called here "unoxidized colloid") and after an exposure to air for 10 s (called here "oxidized colloid"). We observed a violent chemical reaction during air exposure indicated by sparks and a cloud of smoke.

Results and Discussion

A. IR/^{1}H NMR. The main IR bands of the isolated Ti-sol were observed at the following positions in ν [cm^{-1}] = 867(s), 915(vw), 1035(s), 1340(br), 1455(w). Specifically, the absorptions at 1035 and 867 cm^{-1} are assigned to the asymmetric and symmetric C−O−C-bending modes of the cyclic ether. Free THF, in contrast, absorbs at 1070 and 915 cm^{-1}, respectively.

The slight shift of these absorption bands toward lower wavenumbers can be attributed to a higher electron density in the C−O−C-bonding region compared with the free molecule. In any case this shift provides evidence for the presence of intact THF coordinated to the metallic center.

The ^1H NMR investigation of the Ti-sol in [D_8]THF solution yielded two sharp signals at $\delta = 1.77$ and $\delta = 3.61$ (rt, TMS, m, 2H) which are shifted slightly compared with the free molecule THF ($\delta = 1.85$ (bonded to β-C) and $\delta = 3.75$ (bonded to α-C)[14]) which again points to the presence of intact THF interacting with a relatively electropositive center. Note that the mass spectrum of the dry Ti-sol powder ($m/z = 72$, $C_4H_8O^+$) is in agreement with this assignment. Further, the presence of 0.5 mol of THF/mol of Ti in the protonolysis product without any trace of butanol excludes the cleavage of the cyclic ether.

To summarize these investigations, neither the IR nor ^1H NMR spectra gave evidence of Ti-bonded hydrogen. Likewise there is a spectroscopic proof for the remaining THF ring, and there are hints of bonding between the metallic center and the THF ligands.

B. X-ray Photoelectron Spectroscopy. The Ti 2p XP spectrum of the Ti colloid is shown in Figure 1 (lower part). Two spin doublets (Ti $2p_{3/2,1/2}$) representing two different chemical states of Ti can be identified. The peak at lower Ti $2p_{3/2}$ binding energy (BE) (456.2 eV) has a lower intensity compared with the peak at higher BE (458.9 eV).

XPS studies of chemical shifts in Ti 2p spectra have been performed previously for a number of compounds, and these measurements have shown that the Ti 2p BE increases when electronic charge is removed from the Ti atoms. In particular, a correlation between the BE shift and the oxidation number of Ti in the various oxides has been established.[15−19] In order to elucidate the charge state of Ti in the colloid, we compare our XPS results with the corresponding Ti 2p BE of different Ti (sub)oxides and Ti metal.

(8) Anthony, M. T.; Seah, M. P. *Surf. Interface Anal.* **1984**, *6*, 95−107.
(9) "unifit", XPS software, Hesse, R.; Klein, J. University of Leipzig, 1995.
(10) (a) Althoff, K. H.; Drachenfels, W. v.; Dreist, A.; Husmann, D.; Neckenig, M.; Nuhn, H. D.; Schauerte, W.; Schillo, M.; Schittko, F. J.; Wermelskirchen, C. *Part. Accel.* **1990**, *27*, 101−106. (b) Hormes, J. *Phys. Scr.* **1987**, *36*, 36−40. (c) Hormes, J.; Chauvistré, R.; Schmitt, W.; Pantelouris, M. *Acta Phys. Pol. A* **1992**, *82*, 37−50.
(11) Lemonnier, M.; Collet, O.; Depautex, C.; Esteva, J. M.; Raoult, D. *Nucl. Instrum. Methods* **1978**, *152*, 109−111.
(12) Bearden, J. A.; Burr, A. F. *Rev. Mod. Phys.* **1967**, *39*, 125.
(13) Rothe, J.; Franke, R.; Pollmann, J.; Hormes, J.; Bönnemann, H.; Brijoux, W.; Siepen, K.; Richter, J. *Fresenius' J. Anal. Chem.* **1996**, *355*, 372.
(14) Hesse, M.; Meier, H.; Zech, B. *Spektroskopische Methoden in der organischen Chemie* (in German); Thieme Verlag; Stuttgart−New York, 1987.
(15) Ramqvist, L.; Hamrin, K.; Johansson, G.; Fahlman, A.; Nordling, C. *J. Phys. Chem. Solids* **1969**, *30*, 1835−1847.
(16) Lassaletta, G.; Caballero, A.; Gonzalez-Elipe, A. R.; Fernandez, A. *Vaccum* **1994**, *45*, 1085−1086.
(17) Simon, D.; Perrin, C.; Bardolle, J. *Compt. Rend.* **1976**, *C283*, 299−303.
(18) Mayer, J. T.; Giebold, U.; Madey, T. E.; Garfunkel, E. *J. Electron Spectrosc. Relat. Phenom.* **1995**, *73*, 1−11.
(19) Faba, M. G.; Gonbeau, D.; Pfister-Guillouzo, G. *J. Electron Spectrosc. Relat. Phenom.* **1995**, *73*, 65−80.

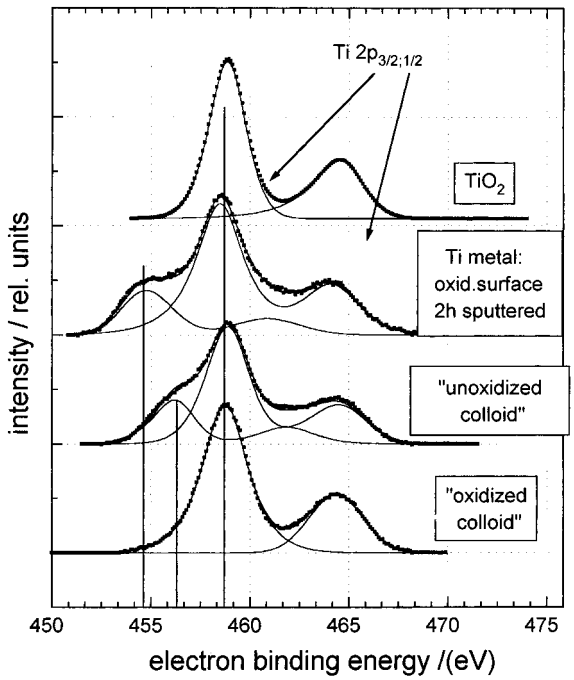

Figure 1. Ti $2p_{3/2,1/2}$ XP spectra of the unoxidized and oxidized Ti colloids, of a sputtered Ti metal surface, and of bulk TiO_2 (anatase). The vertical lines represent the Ti 2p binding energies for Ti metal, the colloidal Ti, and bulk TiO_2.

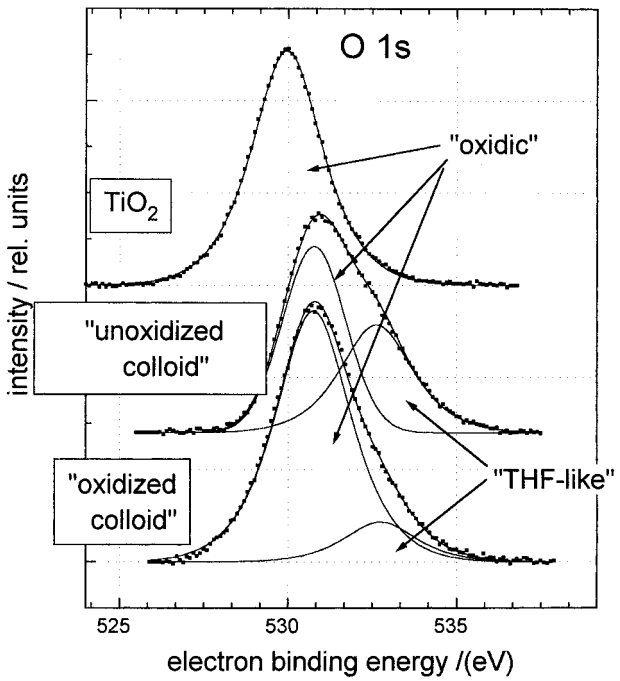

Figure 2. O 1s XP spectra of the unoxidized and oxidized colloids and bulk TiO_2 (anatase). The colloid spectra exhibit two components which are assigned to "oxidic" O atoms (sample-surface) and O atoms bonded in the colloid-coating THF molecules.

Table 1. Electron Binding Energies *E*(O 1s) and *E*(Ti $2p_{3/2}$) of the Unoxidized and Oxidized Ti colloid (10 s of Exposure to Air), Bulk TiO_2 (Anatase), Bulk TiO, Bulk Ti_2O_3, and an Oxidized and a Sputtered Ti Metal Surface[a]

sample	*E*(O 1s)	*E*(Ti $2p_{3/2}$)	ref
unoxidized colloid	530.75	456.2 (colloid)	
	532.6	458.9 (oxide)	
oxidized colloid	530.75	458.75 (oxide)	
	532.75		
Ti metal (oxidized surface)	530.0	458.5 (oxide)	
Ti metal (sputtered for 2 h)	531.0	454.75 (metal)	
		457.4 (oxide)	
Ti metal (sputtered for 4 h, cleaned surface)		454.5 (metal)	453.4,[17] 453.6,[41] 453.8,[15,38] 453.9,[40] 454.1[18,39]
TiO		455.6	454.8,[15] 455.3[17]
Ti_2O_3		456.0	
TiO_2	529.9	458.65	458.5,[16] 458.7,[15,19] 458.8,[17,39] 459.3;[18] O 1s: 530.0[19]

[a] The values are referenced to the Au $4f_{7/2}$ energy (84.0 eV) from an admixture of gold powder and from the sample holder (Ti metal sample), respectively. Values are given in electronvolts. Estimated error ±0.1.

We first consider the Ti 2p spectrum of bulk TiO_2 (anatase). As can be seen (Figure 1, Table 1) the Ti $2p_{3/2}$ energy (458.65 eV) agrees with that of the high BE peak found in the unoxidized colloid. Thus, the Ti 2p signal of the colloid with larger intensity can be assigned to oxidized Ti comparable with that in TiO_2.

The low BE signal at 456.2 eV can now be supposed to represent the chemical state of colloidal [Ti·0.5THF]. It was observed that Ar sputtering of the sample leads to an increasing intensity of this peak relative to the high BE peak (TiO_2). We conclude that the Ti oxide is mainly localized at the "macroscopic" sample surface, i.e., not the colloid-particle "surface", reflecting the extreme affinity of the Ti colloid to residual oxygen or water present in the preparation instrumentation. The TiO_2-like XPS signal is predominant in the spectrum of the unoxidized colloid due to the high surface sensitivity of XPS.

For comparison, Figure 1 also shows the Ti 2p XP spectrum of a polished metal sample recorded after 2 h of Ar sputtering. It can be clearly seen that the low BE doublet representing Ti metal has a lower Ti $2p_{3/2}$ BE (454.75 eV) compared with the colloid (Table 1). The resulting colloid−bulk metal chemical shift amounts to 1.7 eV.

In other words, the Ti 2p BE of the Ti colloid signal (456.2 eV) lies between the values of Ti metal (454.75 eV) and TiO_2 (~458.5 eV). Several authors have reported Ti 2p BE in suboxides differing only slightly from that of the Ti metal (see e.g. ref 19 and the data given in Table 1). The results of our own Ti 2p XPS measurements of commercially obtainable TiO and Ti_2O_3 are also listed in Table 1.

From the comparison of the whole of the Ti 2p BE obtained from oxides, metal, and the colloid, a very similar charge state of colloidal Ti and Ti in suboxides with an oxidation number of +2 and +3, respectively, could be supposed. It is important to state that we have found evidence for the assignment of nonoxidized Ti to the low BE signal in the colloid spectrum.

First, it should be mentioned that oxides with lower Ti oxidation numbers (+2, +3) are more stable in air and do not react with the observed violence under air exposure. As can be easily seen from the Ti 2p spectrum of the oxidized colloid (Figure 1), air exposure leads to the disappearance of the component at 456.2 eV assigned to the colloid itself and to an increasing Ti 2p peak intensity of the TiO_2-like signal at 458.75 eV.

Moreover, the quantitative analysis of both the changes of the Ti 2p and O 1s XPS signals taking place under air exposure supports the presence of colloidal Ti^0 in the unoxidized colloid. We observed slightly different O 1s spectra for the unoxidized and oxidized colloids (Figure 2), both composed of two peaks. The O 1s signal with low BE is assigned to Ti oxide because of the similarity of the O 1s BE (530.75 eV) with the O 1s spectrum measured in TiO_2 (529.9 eV) (Table 1). Assuming

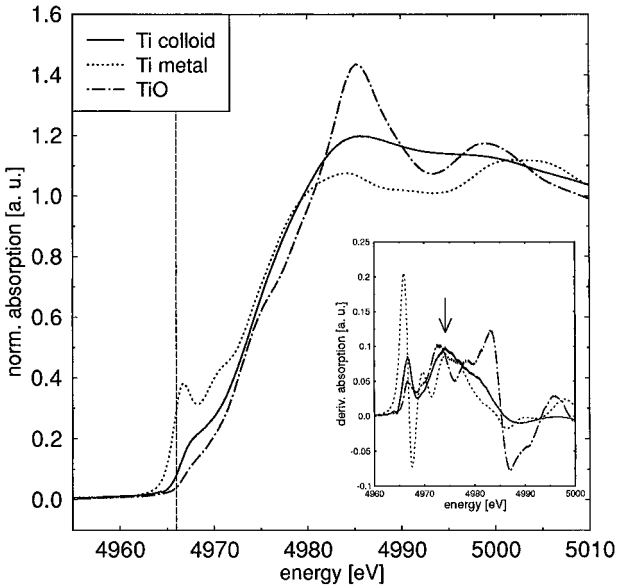

Figure 3. Ti K-XANES spectra of the unoxidized colloid, Ti metal, and crystalline TiO. The vertical dashed line at 4966 eV corresponds to the fist inflection point in the Ti K-XANES spectrum of the pure metal. The appropriate derivative spectra are shown in the inset.

Table 2. Ti $2p_{3/2,1/2}$ (Colloid-Like and TiO_2-Like) and O 1s (THF-Like and TiO_2-Like) Peak Areas in the Unoxidized and Oxidized Colloid and Their Relative Changes during Exposure to Air Determined by Means of Curve Fitting[a]

	Ti 2p		O 1s	
sample	$Ti^{(0)}$·0.5THF	TiO_2	TiO_2	THF
unoxidized colloid[b]	33780	89100	118310	84830
oxidized colloid[b]		123170	204980	31460
oxidized:unoxidized ratio[c]		1.38	1.73	0.37

[a] The determined changes support the presence of nonoxidized Ti^0 particles in the unoxidized colloid and the formation of TiO_2 during the air exposure. [b] Estimated error ±2%. [c] Estimated error ±0.04.

that the Ti particles are surrounded by intact THF ligands, the O 1s peak at higher BE (532.6−532.75 eV) is attributed to THF O atoms. The latter ones have stronger electronegative bonding partners (C, 2.55) in comparison with oxygen in TiO_2 (Ti, 1.54),[20] giving rise to a less negative oxygen charge state in the THF rings indicated by the higher O 1s BE. The intensity of the TiO_2-like O 1s signal is increased after air exposure in contrast to the THF-like O 1s signal.

We investigated whether the increasing intensities (unoxidized → oxidized colloid) of the particular O 1s (low BE) and Ti 2p (high BE) peaks, both representing TiO_2, are correlated. The corresponding peak areas which are proportional to the elemental concentration in the investigated sample region are listed in Table 2. The ratios obtained from the spectra of the oxidized and the unoxidized colloids are given in the lower row of Table 2. We conclude from the different increase of the oxide signal intensities (Ti 2p and O 1s) that the oxidation of zerovalent Ti (Ti^0) to TiO_2 takes place. It can be seen that nearly two ($1.92 = (1.73 - 1)/(1.38 - 1) \approx 2$; see the values in Table 2) O atoms per Ti atom are required to form the finally occurring TiO_2 in the oxidized colloid. If a Ti suboxide would be oxidized to TiO_2, a ratio of $n = 1$ for TiO and $n = 0.5$ for Ti_2O_3, respectively, is necessary. The result of this quantitative analysis is a strong indication that the low BE Ti 2p signal in the spectrum of the unoxidized colloid represents Ti^0.

The colloid−bulk metal BE shift (1.7 eV) has to be explained, because both chemical states in the metal and the colloid are described by Ti^0. This can be done in two different ways. First, the analysis of the observed BE shift in terms of chemical shift points to a strong bonding interaction between the Ti particles and the THF ligands, accompanied by a polarization or a transfer of valence charge from Ti to THF. This can be understood by a comparison of Pauling's electronegativities of Ti (1.54), O (3.44), and C (2.55).[20] The strong interaction is supported by the IR and ^{1}H NMR results and the observation that there is no release of THF molecules at temperatures below 370 K. Second, it is well known from XPS investigations of metal clusters that a small particle size gives rise to significant changes in the electronic structure compared to the bulk metal rationalized by initial- and final-state effects.[21] These size effects also increase the corresponding core-level BE. A more detailed investigation of such contributions to the Ti 2p BE shift in the Ti colloid, based on the Ti Auger parameter[22] and the Ti $L_{2,3}$-XANES,[23] supports a considerable relaxation energy as well as an initial-state contribution to the observed bulk metal−colloid BE shift.

C. X-ray Absorption Near Edge Structure. The Ti K-XANES spectra of the Ti colloid and the reference Ti metal and TiO are presented in Figure 3. The derivatives of the absorption curves are plotted as an inset to this figure. The Ti K-XANES of these samples are characterized by a series of local maxima above the rising edge positioned at ∼4975 eV and a distinct pre-edge feature at ∼4967 eV. In the spectrum of the Ti colloid (solid line) the observed resonances are less pronounced compared with the metal spectrum (dotted line).

The fitting of such spectra to determine the energies of distinct resonances and the absorption edge itself is very difficult. Thus, we consider the corresponding inflection points (XANES) given by the maxima in the first derivatives. We observe significant differences in the energy positions and the intensities of both the pre-edge features and the rising edge between the spectra in Figure 3.

We have found that the derivative spectra of the Ti colloid and Ti metal coincide in the position of the maximum at 4974.2 eV (indicated by an arrow), reflecting equal positions of the inflection points of the appropriate rising edges. From this result we conclude a similar energy position of the absorption edge pointing to the presence of Ti^0 in the colloid as in the metal.

Now, we consider the pre-edge peak of the metal spectrum (dotted line). It is well known for 3d metals that their valence band contains important contributions of p-symmetry states.[24] Consequently, a band-mixing (hybridization) of p- and d-like states in the conduction band is probable. Thus, the pre-edge peak at the rising edge of Ti metal (Figure 3) represents an electronic transition from the Ti 1s level into the lowest unoccupied electronic state which is a 3d-like state. According to the selection rules for X-ray transitions an admixture of the p-like states is required to explain the sharp, otherwise dipole-forbidden, resonance. In the case of the Ti colloid, this band-mixing appears to be less pronounced, resulting in a pre-edge feature of lower intensity visible as a shoulder of the rising edge (solid line). Accordingly the diminished admixture of d-symmetry states with the p-band above the Fermi level can be responsible for the higher absorption intensity above the rising edge in the colloid spectrum, representing Ti 1s → 4p electronic transitions.

(20) Allred, A. L. *J. Inorg. Nucl. Chem.* **1961**, *17*, 215−232.

(21) (a) Mason, M. G. *Phys. Rev. B* **1983**, *27*, 748−762. (b) Wertheim, G. *Z. Phys. D* **1989**, *12*, 319−326.

(22) (a) Wagner, C. D. *Faraday Discuss. Chem. Soc.* **1975**, *60*, 291−300. (b) Thomas, T. D. *J. Electron Spectrosc. Relat. Phenom.* **1980**, *20*, 117−125.

(23) Franke, R.; Pollmann, J.; Rothe, J.; Hormes, J. Unpublished results.

(24) Meisel, A.; Leonhardt, G.; Szargan, R. *Röntgenspektren und Chemische Bindung*; Akademische Verlagsgesellschaft: Leipzig, 1977.

Obviously the energy position of the first inflection point, as a comparable measure of the energy position of the pre-edge feature in the spectrum of the colloid (4966.7 eV), is shifted about 0.7 eV to higher energies compared with Ti metal (4966.0 eV). We note that this shift agrees with the one stated for Ti^{2+} in crystalline TiO with reference to Ti metal, as can be seen in the inset of Figure 3 (compare the solid line with the dashed−dotted line).

In general, the pre-edge feature in Ti K-XANES spectra of Ti oxides is attributed to electronic transitions from the Ti 1s level into empty Ti 4p3d hybridized states overlapping with O 2p orbitals.[25] In particular this resonance underlies the crystal field splitting as will be shown in the discussion of the XANES obtained from the oxidized colloid. The question arising is whether the empty electronic states responsible for the pre-edge feature in the spectrum of the colloid contain some O 2p character owing to an interaction of the Ti atoms with the coating THF molecules or whether they have the same character as in the metal. Note that we failed to simulate the spectrum of the colloid by a superposition of the normalized spectra of Ti metal and Ti oxides which indicates the presence of a distinctive chemical state of the absorbing Ti atoms in the colloid sample.

In principle, the observed shift of the pre-edge peak in the colloid compared with Ti metal can be explained in two different ways. First, a physical origin of this shift can be due to an increased localization of unoccupied electronic states in the colloid as expected when the transition from bulk metal to metal atoms is considered[26] (size effect). The fact that this shift (0.7 eV) is smaller than the recently discussed Ti 2p core-level BE shift (1.7 eV) points to the importance of the extra-atomic relaxation energy effect in the observed XPS bulk metal−colloid shifts in contrast to XANES feature shifts.[21] Second, the higher transition energy observed in the colloid can be caused by the influence of the THF molecules coating the Ti particle. The bonding of intact THF to the metallic center was proven by the IR and ^{1}H NMR measurements, as discussed above. Moreover, our EXAFS results also indicate O as nearest neighbors (next section). Thus, it can be assumed that, upon the formation of the colloid, THF molecules are interacting with Ti^0 particles via Ti 3d and O 2p orbitals, resulting in the formation of p−d states. This may explain the weak, otherwise dipole forbidden, pre-edge absorption observed even in the spectrum of the Ti colloid, where in contrast to the metal obviously no band structure has been formed.

The interaction of Ti atoms with THF gives rise to the shift of the pre-edge structure to an energy position coinciding with the position of the pre-edge structure in the case of TiO (Figure 3). According to our assumption, the charge state of the Ti atoms in the colloid is not strongly affected by these bonds.[27] As a result, a similar position of the rising edge can be found compared with the metal. It should be noted that it is obviously impossible to distinguish between "particle−surface" and "particle−bulk" Ti atoms.

In order to investigate the nature of the pre-edge feature and to separate the different influences (THF-bonding, particle size) of the XANES (and XP) spectra, it is necessary to investigate naked clusters with different sizes and colloids with different ligands. However, the preparation of these particles is very difficult and was not successful up to now.

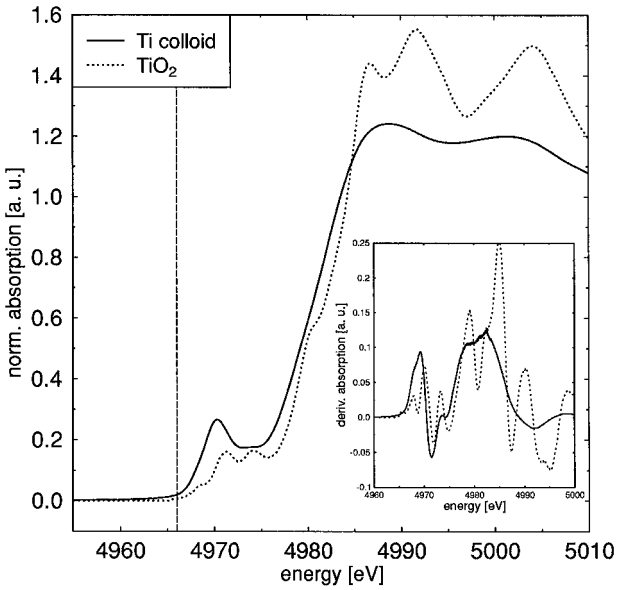

Figure 4. Ti K-XANES spectra of the oxidized colloid after air exposure and TiO_2 (rutile). The appropriate derivative spectra are shown in the inset.

To finish the XANES discussion, it is quite interesting to have a look at the spectrum of the oxidized colloid. In Figure 4 XANES spectra of the oxidized colloid and TiO_2 are presented; again the first derivatives are plotted as an inset. The dramatic changes in the spectral features occurring between the unoxidized colloid and the oxidized colloid, especially the shift of the rising edge position to higher energies (∼5 eV), indicate the formation of a Ti oxide with an atomic structure quite different from bulk TiO_2. The inflection point at 4982.3 eV of the oxidized colloid absorption curve (solid line, Figure 4) coincides with the shoulder in the spectrum of rutile (dotted line). This observation is a strong hint of the formation of Ti^{4+} during air exposure of the Ti colloid as was also observed in the XP spectra.

The pre-edge structures are known to be very sensitive to the coordination symmetry of Ti in its oxidized state.[25] In the literature, the second and third pre-edge peaks are attributed to the transitions Ti 1s → t_{2g} and e_g MO states, respectively, which are created from Ti 3d and O 2p states under the influence of the crystal field.[25] The origin of the first peak is still a matter of debate. The weak pre-edge structures of bulk TiO_2 reflect a 6-fold coordination of Ti in a distorted oxygen octahedron. In contrast, the XANES spectrum of Ti in tetrahedral coordination as e.g. in Ba_2TiO_4 reveals only one strong pre-edge feature at slightly lower energy compared with the second pre-edge peak of rutile.[28] Taking the absence of inversion symmetry into account, this peak is attributed to the dipole allowed Ti 1s → t_2 transition. Considering the intensive peak observed at 4970.2 eV in the XANES spectrum of the oxidized colloid (1s → t_{2g} in rutile at 4971.1 eV), the formation of Ti^{4+} in a distorted octahedral coordination may be assumed.

Note that the XANES spectrum of the unoxidized colloid obtained in the standard transmission mode gives no support for the presence of TiO_2 in contrast to the XPS results. This observation confirms our conclusion derived by XPS results that Ti is not oxidized in the bulk of the colloid sample during the synthesis but that TiO_2 is located on the macroscopic surface of the sample.

(25) Waychunas, G. A. *Am. Mineral.* **1987**, *72*, 89−101.
(26) Arp, U.; Lagutin, B. M.; Materlik, G.; Petrov, I. D.; Sonntag, B.; Sukhorukov, V. L. *J. Phys. B* **1993**, *26*, 4381−4398.
(27) Barbonneau, F.; Doeuff, S.; Leaustic, A.; Sanchez, C.; Cartier, C.; Verdaguer, M. *Inorg. Chem.* **1988**, *27*, 3166−3172.
(28) Yarker, C. A.; V. Johnson, P. A.; Wright, A. C.; Wong, J.; Gregor, R. B.; Lytle, F. W.; Sinclair, R. N. *J. Non-Cryst. Solids* **1986**, *79*, 117−136.

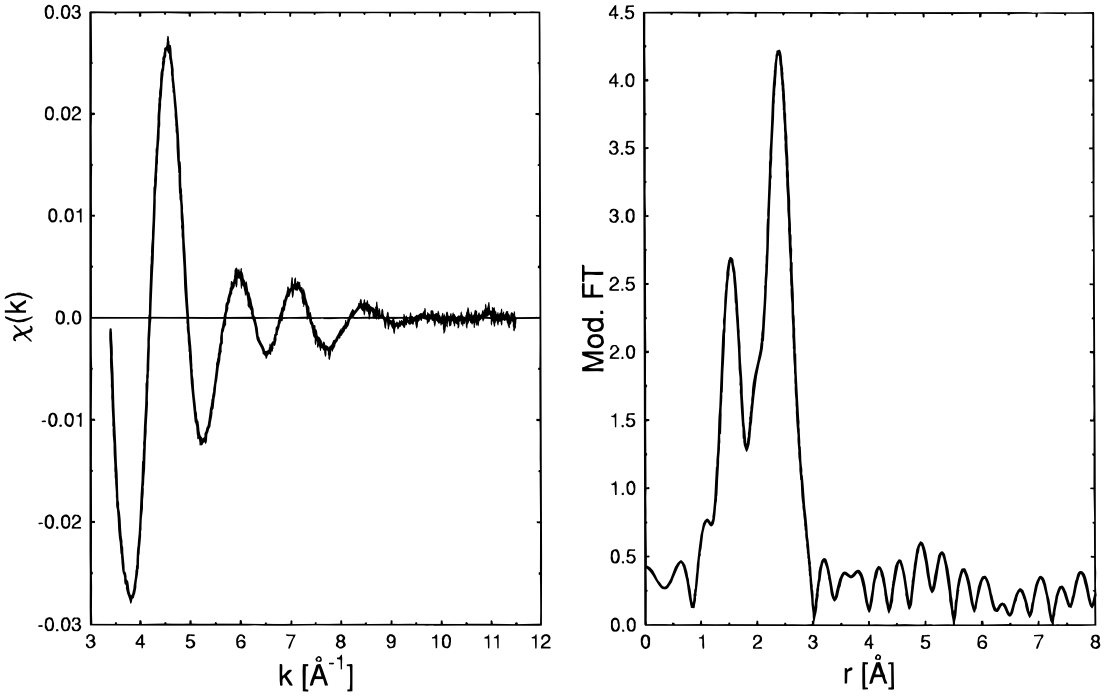

Figure 5. (a, left) Normalized EXAFS function $\chi(k)$ of the unoxidized colloid. (b, right) Fourier transform of the k^3-weighted $\chi(k)$ function of the unoxidized colloid.

Table 3. Fit Parameters for FEFF Simulation (Ti K-EXAFS Analysis)[a]

shell	back-scatterer	distance[b] (Å)	coordination number[c]	σ^2 [d] (Å^2)	ΔE_0[e] (eV)
1	O	1.96	0.8	0.015	−2.0
2	Ti	2.83	1.8	0.009	4.0

[a] σ^2 = Debye−Waller factor. ΔE_0 = relative shift of the absorption edge between experiment and phase fit. [b] Estimated error ±0.01. [c] Estimated error ±0.1. [d] Estimated error ±0.002. [e] Estimated error ±1.

D. Extended X-ray Absorption Fine Structure. EXAFS analysis has been performed following the standard method, by the least-squares fitting of the Fourier-filtered EXAFS function in *k*-space, using a program package developed by Ertel et al.[29] Figure 5a shows the EXAFS function $\chi(k)$ derived after the pre-edge fit procedure and normalization to an atomic background function. The sample thickness has been optimized to achieve an edge jump of 1.5 in order to avoid any reduction of the EXAFS amplitude by the thickness effect.[30]

In the Fourier transform (Figure 5b) of the k^3-weighted EXAFS function $\chi(k)$ (3.5−11.5 Å^{-1}) (Figure 5a) a double peak with maxima around 1.6 and 2.4 Å, respectively, can be seen (so far, the phase shift in $\chi(k)$ is not considered), whereas no signal from back-scatterers at distances above 3 Å can be detected. Consequently, Fourier-filtering of the EXAFS data was performed in the range of 0.8−3.2 Å.

Assuming a bonding of THF to the Ti clusters via Ti−O interaction, the first peak in the Fourier spectrum of $\chi(k)$ can be attributed to an O back-scatterer. Recently, a Ti−O distance of 1.8 Å has been found in Ti alkoxides,[27] whereas the first O neighbor in rutile is situated at 1.95 Å.[31] Theoretical phase shifts and amplitude functions calculated by a modification of the program code FEFF (V3.1)[32] have been employed in the fit procedure of Ertel,[29] using the metal value for the Ti−Ti distance (2.92 Å) and the rutile value for the Ti−O distance (1.95 Å) as input parameters.

The best fit to the Fourier−filtered $\chi(k)$ function (Figure 6a) is obtained by simultaneously adjusting the parameters for both shells. This procedure is justified to the total data range in *k*-space and the width of the filtering window employed in the analysis. The best fit parameters are listed in Table 3. The error margins have been estimated following the method suggested by Teo.[33] In Figure 6b the fit compared to the Fourier transform of the filtered dats is presented.

Our EXAFS results can be seen as a further hint of a structural model for colloidal [Ti·0.5THF] which is based on small particles consisting only of a few Ti atoms. According to this model, the THF molecules are bonded through O atoms. The Ti−Ti distance of 2.83 Å derived from EXAFS is somewhat smaller than the corresponding bulk values for the first shell (in the Ti hexagonal close-packed (hcp) crystal the next neighbors are found at two slightly different distances, 2.95 and 2.89 Å[34]). Such a decrease of bond distances in the case of small metallic clusters compared to bulk metals has already been reported for other systems.[35]

The Ti−O distance of 1.96 Å nearly agrees with that found in TiO_2 (1.95 Å). Considering the low coordination numbers of Ti and O with a Ti:O ratio of ∼2.5 as well as the absence of higher coordination shells, the possibility of simulating the χ-(k) funktion by means of the multiple scattering code FEFF (V6.0)[32] has been checked as the last step of EXAFS analysis. The Ti−Ti and Ti−O distances as derived from the EXAFS analysis have been employed for the calculations.

Using the coordinates of a regular Ti_{13} cluster (as a fraction of an hcp structure) and six O atoms in octahedral configuration around Ti as input parameters, the mismatch in phase and

(29) Ertel, T. S.; Bertagnolli, H.; Hückmann, S.; Kolb, U.; Peter, D. *Appl. Spectrosc*. **1992**, *46*, 690−698.
(30) (a) Parrat, L. G.; Hempstead, C. F.; Jossem, E. L. *Phys. Rev*. **1957**, *105*, 1228−1232. (b) Stern, E. A.; Kim, K. *Phys. Rev. B* **1981**, *23*, 3781−3786.
(31) Schulz, E.; Ferrini, C.; Prins, R. *Jpn. J. Appl. Phys*. **1993**, *32*, 490−492.
(32) Rehr, J. J. *Jpn. J. Appl. Phys*. **1993**, *32*, 8−12.
(33) Teo, B. K. *EXAFS: Basic Principles and Data Analysis*; Springer Verlag: Berlin−Heidelberg−New York−Tokyo, 1986.
(34) Schulze, G. E. R. *Metallphysik*; Akademieverlag GmbH: Berlin, 1976; pp 51−55.
(35) Clausen, B. S.; Topsoe, H. *Jpn. J. Appl. Phys*. **1993**, *32*, 95−98.

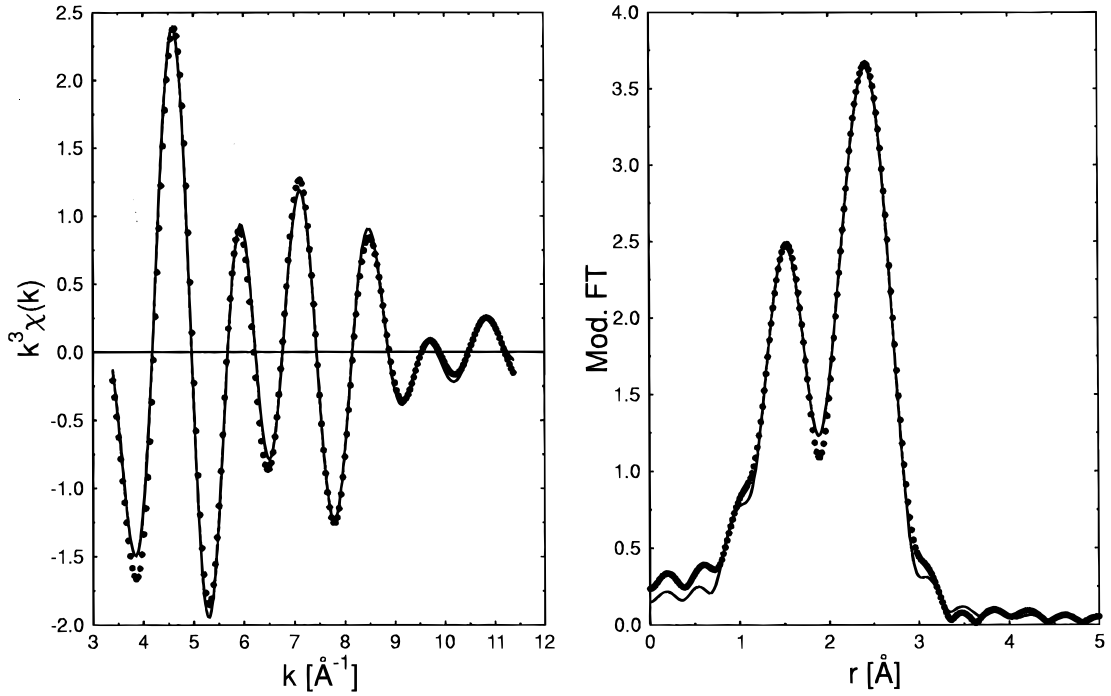

Figure 6. Ti K-EXAFS analysis of the (a, left) unoxidized colloid: line = Fourier-filtered $\chi(k)$ (range of 0.8−3.2 Å, k^3-weighted), dots = best fit. (b, right) Ti colloid: line = Fourier transform of filtered $\chi(k)$, dots = Fourier transform of the best fit.

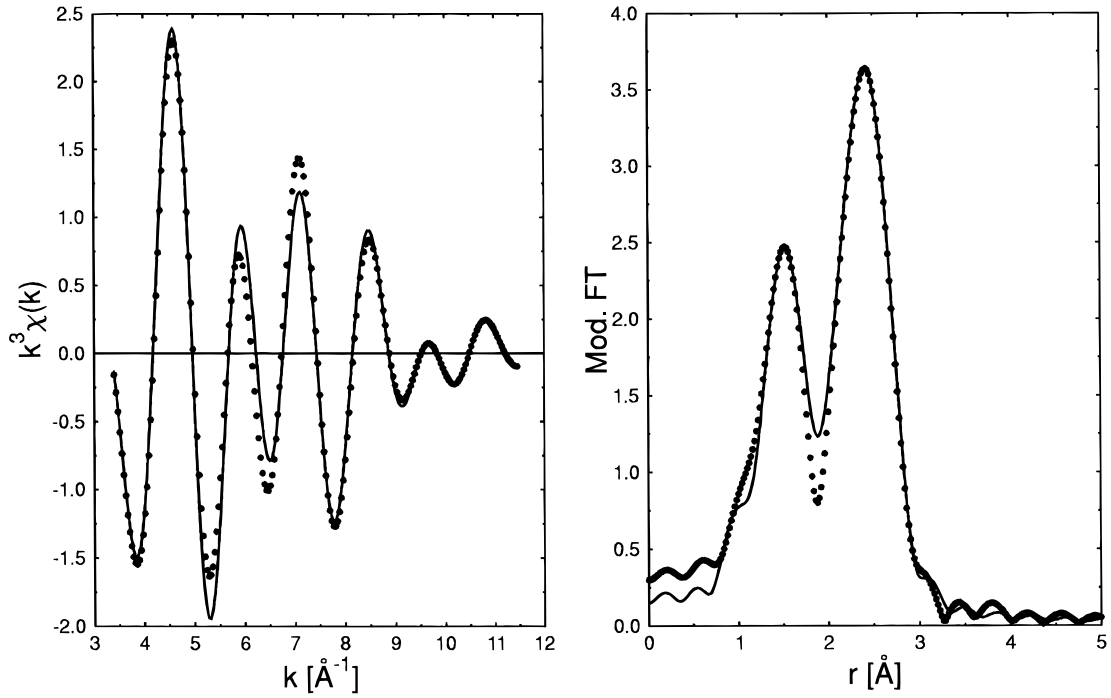

Figure 7. Ti K-EXAFS analysis of the (a, left) unoxidized colloid: line = Fourier-filtered $\chi(k)$ (range 0.8−3.2 Å, k^3-weighted), dots = simulation by the FEFF program code. (b, right) Ti colloid: line = Fourier transform of filtered $\chi(k)$, dots = Fourier transform of the simulation by the FEFF computer program code.

amplitude ratio between experiment and simulation was obvious, if the calculation was performed for the central Ti atom. Starting with one of the 12 Ti atoms of the first full shell and only considering its three next neighbors as well as an additional O atom in a 3-fold coordination (Figure 8), good agreement in phase and amplitude was achieved. Parts a and b of Figure 7 show the corresponding simulation results in *k*- and *r*-space, respectively. An amplitude reduction factor of 0.92 and σ^2 values of 0.010 and 0.016 Å^2, for Ti−O and Ti−Ti pairs, respectively, were employed in the calculation.

The absence of a higher Ti coordination shell in the experimental data, which should be visible for the outer Ti atoms of a full-shell cluster, as well as the low average Ti−Ti coordination number of ∼1.8, may be due to structural disorder of the back-scattering atoms, which is known to be a major limitation of standard EXAFS analysis in the case of small metal clusters.[36]

In a previous EXAFS investigation of a Ti colloid, back-scattering from higher coordination shells was observed and a much larger Ti−Ti distance (2.96 Å) than reported here was found.[1a] The discrepancy in the Ti−Ti distance may be

(36) (a) Schmid, G. *Cluster and Colloids*, VCH: Weinheim, 1994; p 43. (b) Montano, P. A.; Shenoy, G. K.; Alp, E. E.; Schulze, W.; Urban, J. *Phys. Rev. Lett.* **1986**, *56*, 2076−2079.

explained by the high amount of residual hydrogen in the colloid sample investigated in ref 1a before the improvement of the preparation method.[2] Although back-scattering of photoelectrons by hydrogen neighbors is too weak to be detected directly by EXAFS, hydrogen may cause a significant lattice expansion.[37] The KCl impurities reported for the earlier investigated sample and their possible effect on the structure of colloidal particles are assumed to be responsible for the observed back-scattering from higher coordination shells.

Conclusions

The NMR, IR, EDX, and HRTEM analysis of $[Ti{\cdot}0.5THF]_x$ (**1**) has shown that this colloid consists of very small metallic particles coordinated to intact THF ligands. The examination of this colloid by means of XPS supports the presence of nonoxidized Ti particles (besides oxidized areas at the surface of the sample). The observed chemical shift of the Ti 2p BE compared with Ti metal (1.7 eV) may be explained by a considerable bonding interaction accompanied by a charge transfer or polarization to the coordinated THF molecules as well as physical particle-size effects on the core-level BE. XANES spectra of the colloid and reference samples gave evidence for the presence of Ti^0 particles having a poorly developed electronic band structure compared with Ti metal. The significant energy shift of the pre-edge resonance in the Ti K-shell XANES spectrum points to a bonding interaction between Ti atoms and THF molecules via O 2p−Ti 3d orbitals. EXAFS simulations assuming a fraction of a full-shell Ti_{13} cluster surrounded by O atoms showed good agreement with the experimentally observed data. From these data relatively small Ti−Ti distances (2.83 Å) compared with those of Ti metal (2.89−2.95 Å) are derived. The derived Ti−O distance of 1.96 Å indicates a rather strong Ti−THF interaction which is consistent with the results of XPS, XANES, and thermolysis experiments. All these analytical results may be visualized by the proposed structural model of the Ti colloid **1** presented in Figure 8.

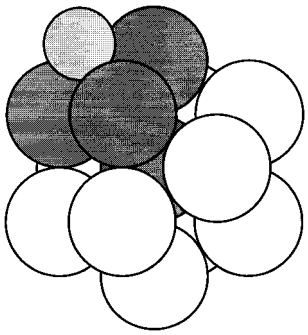

Figure 8. A proposed structural model for the investigated Ti colloid based on a regular Ti^0_{13} cluster (dark gray, Ti atoms as input for the FEFF simulation; light gray, THF O atom).

Acknowledgment. We gratefully acknowledge the BMBF, Bonn, for financial support under Contract No. 03 D 0007 A2, the Fonds der Chemischen Industrie e.V., Frankfurt/M., the Deutsche Forschungsgemeinschaft (DFG), Bonn, and Mr. I. Brock (Bonn University) for reading the paper.

JA953525D

(37) Lengeler, B. *Solid State Commun.* **1985**, *55*, 679−682.
(38) Zhao, L. Z.; Liu, S. H.; Wang, D. H.; Pan, C. H. *J. Electron Spectrosc. Relat. Phenom.* **1990**, *52*, 571−580.
(39) Wagner, C. D.; Riggs, W. M.; Davis, L. E.; Moulder, J. F.; Muilenberg, G. E. *Handbook of X-ray Photoelectron Spectroscopy*; Perkin-Elmer Corp.: Eden Prairie, 1975.
(40) Wagner, C. D.; Gale, L. H.; Raymond, R. H. *Anal. Chem.* **1979**, *51*, 466−475.
(41) Fuggle, J. C.; Mårtensson, N. *J. Electron Spectrosc. Relat. Phenom.* **1980**, *21*, 275−281.